In situ calibration of the foil detector for an infrared imaging video bolometer using a carbon evaporation technique

メタデータ	言語: English 出版者: 公開日: 2021-10-29 キーワード (Ja): キーワード (En): 作成者: MUKAI, Kiyofumi, PETERSON, Byron J., TAKAYAMA, Sadatsugu メールアドレス: 所属:
URL	http://hdl.handle.net/10655/00012660

This work is licensed under a Creative Commons Attribution 3.0 International License.

In-situ calibration of the foil detector for an infrared imaging video bolometer using a carbon evaporation technique[a)]

K. Mukai,[1,2,b)] B. J. Peterson,[1,2] S. Takayama,[1] and R. Sano[3]

[1]*National Institute for Fusion Science, National Institutes of Natural Sciences, Toki 502-5292, Japan*
[2]*SOKENDAI (The Graduate University of Advanced Studies), Toki 502-5292, Japan*
[3]*National Institutes for Quantum and Radiological Science and Technology, Naka 311-0193, Japan*

(Presented XXXXX; received XXXXX; accepted XXXXX; published online XXXXX)
(Dates appearing here are provided by the Editorial Office)
The InfraRed imaging Video Bolometer (IRVB) is a useful diagnostics for the multi-dimensional measurement of plasma radiation profiles. For the application of IRVB measurement to the neutron environment in fusion plasma devices such as the Large Helical Device (LHD), in-situ calibration of the thermal characteristics of the foil detector is required. Laser irradiation tests of sample foils show that the reproducibility and uniformity of the carbon coating for the foil was improved using a vacuum evaporation method. Also, the principle of the in-situ calibration system was justified.

I. INTRODUCTION

InfraRed imaging Video Bolometers (IRVBs) have been installed in LHD [1, 2], JT-60U [3], HL-2A [4], and KSTAR for the measurement of plasma radiation profiles to investigate phenomena such as plasma detachment [5]. The fundamental schematic of an IRVB is a combination of a pinhole camera and an IR camera [see, FIG. 1]. The profiles of the plasma radiation are collimated by an aperture (e.g., 8 mm × 8 mm) in the pinhole camera and are projected onto a thin platinum foil (e.g., 130 mm × 100 mm, t = 2.5 μm) as a two-dimensional temperature distribution. Here, the heat-diffusion effect of the foil must be considered to estimate the radiation profile from the IR image using the two-dimensional heat diffusion equation [1]. Therefore, the local thermal characteristics, emissivity, ε, thermal conductivity, k, foil thickness, t_f, and thermal diffusivity, κ should be calibrated over all the bolometer pixels (~1,000) on the foil.

An in-situ calibration technique of these heat characteristics was developed in JT-60U [6]. However, the neutron irradiation effect has not been investigated although it should be investigated for the application of the IRVB measurement to the neutron environment of deuterium plasma experiments in the Large Helical Device (LHD) and other magnetically confined plasma devices. Moreover, the calibration technique was advanced enough to be able to evaluate local parameters [7, 8]. Then, an upgraded in-situ calibration system was designed [9]. In both in-situ calibration systems, a He-Ne laser with a wavelength of 632.8 nm as the known heat source must irradiate the foil from the side opposite of the plasma radiation. Therefore, the carbon coating on both sides of the foil should be carried out with high reproducibility and uniformity. In this paper, the improvement of the carbon coating of the foil using a vacuum evaporation method is reported.

II. SCHEMATIC OF IN-SITU CALIBRATION SYSTEM

The schematic of the in-situ calibration system [9] is shown in FIG. 1. A periscope system must be applied to protect the IR camera detector from damage by the direct irradiation of X-rays, neutrons, and gammas from the plasma. A He-Ne laser (JDS Uniphase/ 1145, 632.8 nm × 22.5 mW), as the known radiation power source, is injected to the foil. Laser irradiation points can be scanned using a mirror with two motorized goniometers (SIGMAKOKI/ GOHTM-40A60/ GOHTM-40A75), which correspond to the center of the each bolometer pixel. The visible laser can be transmitted to the foil and the IR radiation from the foil can be reflected to the IR camera using a hot mirror (Edmund Optics/ #64-472 45° 101 × 127) since it has a transmittance of >

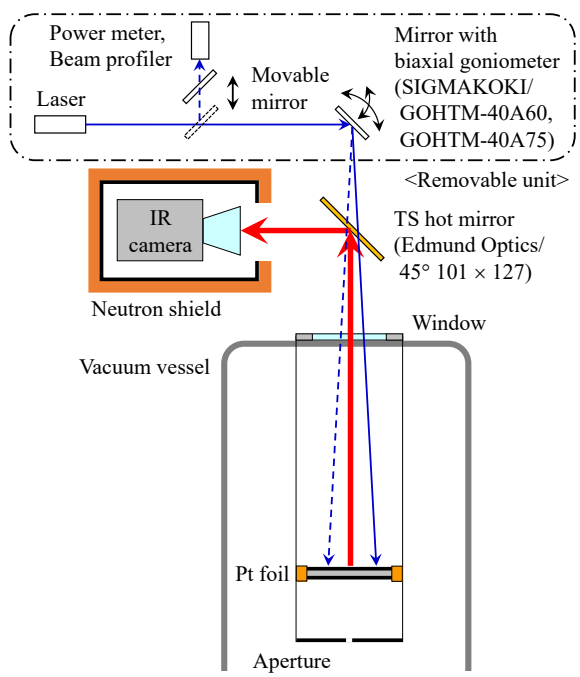

FIG. 1. (Color online). Schematic of the in-situ calibration system for the thermal characteristics of the IRVB foil.

[a)]Contributed (or Invited) paper published as part of the Proceedings of the 21st Topical Conference on High-Temperature Plasma Diagnostics (HTPD 2016) in Madison, Wisconsin, USA.
[b)]Author to whom correspondence should be addressed: mukai.kiyofumi@LHD.nifs.ac.jp

85% for visible light and a reflectance of > 95% for IR signal [10].

III. IMPROVEMENT OF CARBON COATING OF FOIL DETECTOR

The plasma side of the foil detector is coated by carbon to increase the absorption of broadband plasma radiation. The opposite (camera) side is also coated to increase the IR signal radiated to the IR camera. The laser must be irradiated from the camera side in this in-situ calibration system. Then, reproducibility and uniformity are required for the carbon coating on both sides. However, the conventional coating method using carbon spray cannot obtain high reproducibility and uniformity. Therefore, a vacuum evaporation technique was introduced in this study. The schematic of evaporation coating is shown in FIG. 2. A carbon rod is evaporated using resistive heating in vacuum. The evaporated carbon is deposited on a Pt foil. A shutter is used to block the deposition of impurities attached to the carbon rod at the beginning of the evaporation coating.

Small samples of the foil detector were made using ICF 34 gaskets (ϕ = 16.3 mm) as shown in FIG. 3. The platinum foil with a thickness of 2.5 μm was fixed between two foil frames just as in the LHD plasma experiments. The samples were coated on both sides by the spray (Aerodag G) or by the evaporation method (HITACHI/ E-1010). The evaporation coated sample was annealed at 400°C for 30 minutes before coating.

A He-Ne laser (JDS Uniphase/ 1145, 632.8 nm × 12.7 mW) was aimed at the center of the foil samples in a test vacuum chamber. The IR images observed from the side opposite of the laser are shown in FIG. 4. Although a non-uniform structure was observed in the case of the spray coating (FIG. 4 (a)), a concentric circular temperature profile was obtained in the case of the vacuum evaporation coating (FIG. 4 (b)). FIG. 5 shows the temperature profiles comparing the laser irradiation from both sides. While uneven structure and a difference between both sides were observed in the case of the spray coating (FIG. 5 (a)), similar smooth profiles on both sides were obtained with the vacuum evaporation coating (FIG. 5 (b)). To evaluate the difference in the temperature profile between both sides, a pseudo-Voigt function fitting (Eq. 1) was performed

$$\Delta T = \Delta T_0 + A\left[f\frac{2}{\pi}\frac{w}{4(x-x_c)^2+w^2} + (1-f)\frac{\sqrt{4\ln 2}}{\sqrt{\pi}w}\exp\left\{-\frac{4\ln 2}{w^2}(x-x_c)^2\right\}\right]. \quad (1)$$

Here, ΔT_0 is the offset, x_c is the peak center, A is the amplitude, w is

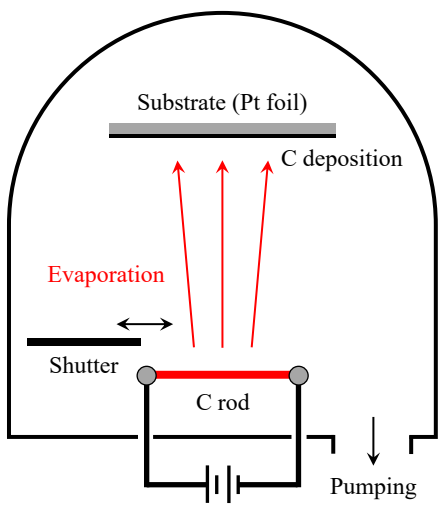

FIG. 2. (Color online). Schematic of evaporation coating.

FIG. 3. (Color online). Platinum foil samples blackened by carbon spray (left) and vacuum evaporation (right).

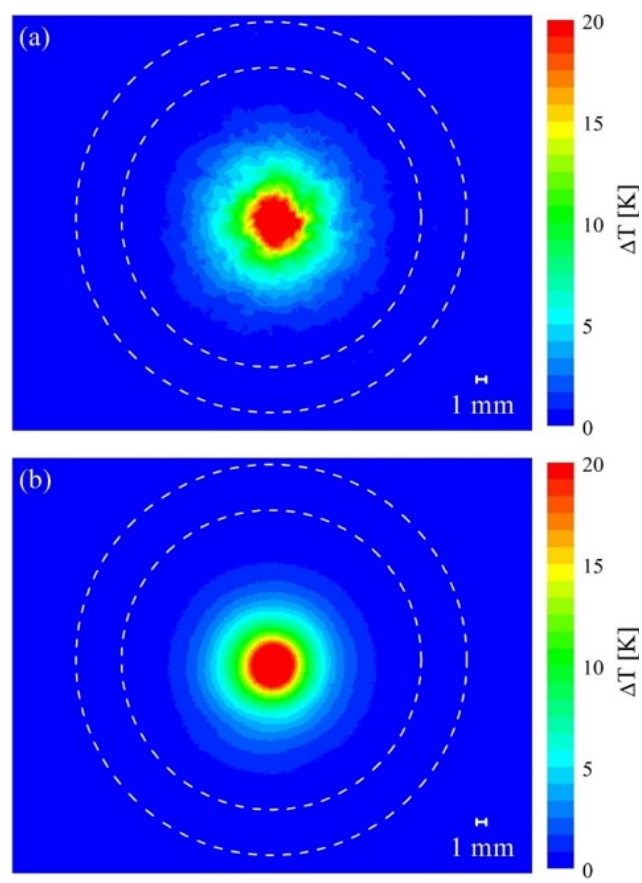

FIG. 4. (Color online). IR images of (a) spray coated and (b) vacuum evaporation coated samples observed from opposite side of the laser irradiation. Color scale indicates the difference of IR intensity after and before the laser irradiation. Dashed lines are foil frame.

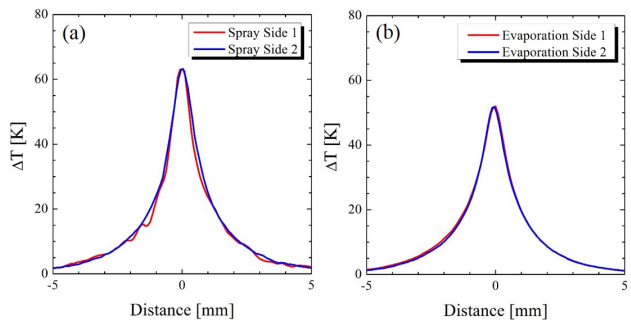

FIG. 5. (Color online). Temperature profile of (a) spray coated and (b) vacuum evaporation coated samples comparing the laser irradiation from both sides. Vertical axis indicates the temperature difference after and before the laser irradiation.

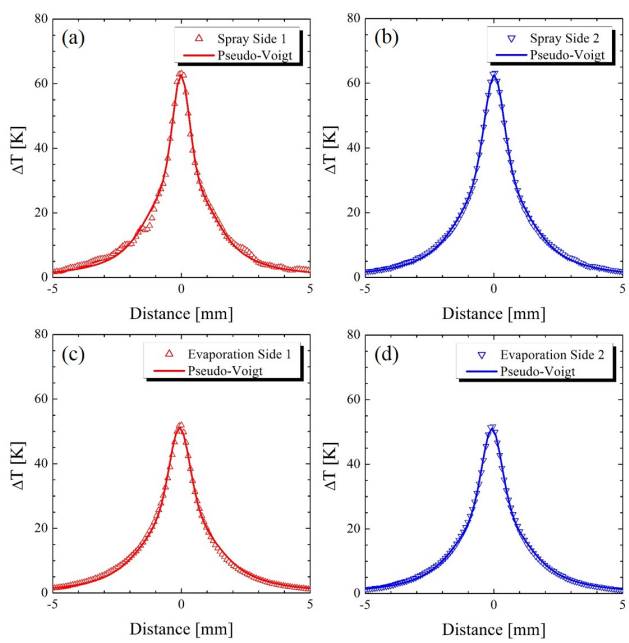

FIG. 6. (Color online). Pseudo-Voigt fitting of the temperature profile of (a), (b) spray coated, and (c), (d) vacuum evaporation coated samples comparing of the laser irradiation from both sides.

TABLE I. Fitting parameters of temperature profiles.

Spray	Side 1	Side 2	Error [%]
Amplitude, A	162.1	175.6	8.00
Width, w	1.32	1.505	13
Offset, ΔT_0	-0.26	-0.48	59
Shape factor, f	1.40	1.319	6
Evaporation	**Side 1**	**Side 2**	**Error [%]**
Amplitude, A	150.4	146.0	3.0
Width, w	1.57	1.527	3
Offset, ΔT_0	-0.50	-0.47	6
Shape factor, f	1.320	1.320	0.000

the width, and f is the profile shape factor. The fitting results are shown in FIG. 6 and TABLE I. The error was evaluated as $|(P_1-P_2) / \overline{P}_i|$ (i = 1, 2 indicates the side of the foil). The amplitude, A, and width, w, of the temperature profile are used for the calibration of the local thermal characteristics. The errors in A and w between both sides were improved from 8.00% to 3.0% and from 13% to 3%, respectively by introducing the vacuum evaporation coating. These results indicate that higher reproducibility and uniformity of the coating can be obtained by the vacuum evaporation coating. Therefore, the vacuum evaporation coating technique can be applied to the in-situ calibration system.

IV. SUMMARY

For the application of the IRVB measurement to the neutron environment in fusion plasma devices such as LHD, in-situ calibration of the thermal characteristics of the foil detector is required. In the in-situ calibration system, the laser must be irradiated from the camera side. Then, reproducibility and uniformity are required for the carbon coating on both sides. In this paper, the characteristics of the carbon coating of the foil were improved by introducing the vacuum evaporation coating technique instead of the conventional spray coating. Laser irradiation tests using small foil detector samples showed that carbon coating with higher reproducibility and uniformity was successfully obtained. Therefore, the principle of the in-situ calibration system was justified.

Moreover, the emissivity was increased from 0.6 to 0.9 using the vacuum evaporation coating by the rough estimation of a radiation pyrometer just after annealing. This result indicates that the S/N ratio of the IRVB measurement will be improved. Through this increased sensitivity and the improved uniformity, a high resolution detector can be realized and a large number of bolometer pixels can be obtained which is required for the tomographic reconstruction using multiple IRVBs.

ACKNOWLEDGEMENTS

This work was supported by NIFS/NINS (NIFS15ULHH026).

[1]B.J. Peterson, A.Yu. Kostrioukov, N. Ashikawa, M. Osakabe, and S. Sudo, Rev. Sci. Instrum. **74**, 2040 (2003).
[2]K. Mukai, B.J. Peterson, S.N. Pandya, R. Sano, and M. Itomi, Plasma Fusion Res. **9**, 3402037 (2014).
[3]B.J. Peterson, S. Konoshima, H. Parchamy, M. Kaneko, T. Omori, D.C. Seo, N. Ashikawa, A. Sukegawa, and JT-60U Team, J. Nucl. Mater. **363-365**, 412 (2007).
[4]J.M. Gao, Y. Liu, W. Li,Z.Y. Cui, Y.B. Dong, J. Lu, Z.W. Xia, P. Yi, and Q.W. Yang., Rev. Sci. Instrum. **85**, 043505 (2014).
[5]K. Mukai *et al*., Nucl. Fusion **55**, 083016 (2015).
[6]H. Parchamy, B.J. Peterson, H. Hayashi, D.C. Seo, N. Ashikawa, and JT-60U Team, Rev. Sci. Instrum. **77**, 10E515 (2006).
[7]R. Sano, B.J. Peterson, E.A. Drapiko, D.C. Seo, Y. Yamauchi, and T. Hino, Plasma Fusion Res. **7**, 2405039 (2012).
[8]S.N. Pandya, B.J. Peterson, R. Sano, K. Mukai, E.A. Drapiko, A.G. Alekseyev, T. Akiyama, M. Itomi, and T. Watanabe, Rev. Sci. Instrum. **85**, 054902 (2014).
[9]K. Mukai, B.J. Peterson, S.N. Pandya, and R. Sano, Rev. Sci. Instrum. **85**, 11E435 (2014).
[10]Edmund Optics Inc. Available at <http://www.edmundoptics.com/optics/optical-mirrors/hot-cold-mirrors/high-performance-hot-mirrors/64472/> [Accessed 20 July 2016]